第 33 卷第 6 期
2017 年 6 月

无 机 化 学 学 报
CHINESE JOURNAL OF INORGANIC CHEMISTRY

Vol.33 No.6
939-946

吡唑双钯(Ⅱ,Ⅱ)配合物的合成与表征及其在 Suzuki 偶联反应中的催化反应

陈 涵[1] 于智淳[2] 邓 威[1] 蒋选丰*,[2] 于澍燕*,[1,2]

([1]中国人民大学化学系,自组装化学实验室,北京 100872)

([2]北京工业大学环境与能源工程学院,绿色催化与分离北京市重点实验室,北京 100124)

摘要:配体 3,5-二(2-吡咯)吡唑(HL)与二硝酸根桥联双钯配合物在溶液中通过配位作用形成了一系列吡唑基双钯(Ⅱ,Ⅱ)夹子 $[Pd_2(bpy)_2L_2]^{2+}$ (**1**)、$[Pd_2(dmbpy)_2L_2]^{2+}$ (**2**)和$[Pd_2(phen)_2L_2]^{2+}$ (**3**)(bpy=2,2′-联吡啶,dmbpy=4,4′-二甲基-2,2′-联吡啶, phen=1,10-菲咯啉)。运用 ^{1}H NMR、^{13}C NMR、ESI-MS 和 X 射线单晶衍射等测试手段对 **1~3** 的结构进行了表征。其晶体结构中存在弱的 Pd…Pd 键(0.303~0.313 nm)相互作用,通过分子间的氢键作用形成一维二重螺旋结构,可作为一种新颖的 Suzuki-coupling 反应的高效催化剂。

关键词:双钯(Ⅱ)夹子;催化;Suzuki 偶联反应

中图分类号:O614.82$^+$3 **文献标识码**:A **文章编号**:1001-4861(2017)06-0939-08

DOI:10.11862/CJIC.2017.090

Pyrazolate-Based Dipalladium (Ⅱ,Ⅱ) Complexes: Syntheses, Characterization and Catalytical Performance in Suzuki-Coupling Reaction

CHEN Han[1] YU Zhi-Chun[2] DENG Wei[1] JIANG Xuan-Feng*,[2] YU Shu-Yan*,[1,2]

([1]*Laboratory for Self-Assembly Chemistry, Department of Chemistry, Renmin University of China, Beijing* 100872, *China*)

([2]*Beijing Key Laboratory for Green Catalysis and Separation, Department of Chemistry and Chemical Industry, College of Environmental and Energy Engineering, Beijing University of Technology, Beijing* 100124, *China*)

Abstract: A series of pyrazolate-based dipalladium(Ⅱ,Ⅱ) complexes named $[Pd_2(bpy)_2L_2]^{2+}$ (**1**), $[Pd_2(dmbpy)_2L_2]^{2+}$ (**2**) and $[Pd_2(phen)_2L_2]^{2+}$ (**3**) (bpy=2,2′-bipyridine, dmbpy=4,4′-dimethyl-2,2′-bipyridine. phen=1,10-phenanthroline) have been synthesized through a directed coordination approach that involves spontaneous deprotonation of the 1*H*-pyrazolyl ligands(HL) in aqueous solution driven by coordination effect. All of new complexes **1~3** have been fully characterized by ^{1}H NMR, ^{13}C NMR, ESI-MS and single-crystal X-ray diffraction analysis. A weak intramolecular Pd…Pd (0.303~0.313 nm) bonding interaction exist in the solid crystal structure, a 1D helical chain network formed by hydrogen bonds interactions between intermolecular, which can be employed as a new kind of high-efficiency catalysts for Suzuki-coupling reaction . CCDC: 1519041, **1**·2PF_6^-; 1536149, **2**·2PF_6^-; 1536150, **3**·2PF_6^-.

Keywords: dipalladium(Ⅱ) clips; catalyst; Suzuki-coupling reaction

收稿日期:2016-12-24。收修改稿日期:2017-03-13。

国家自然科学基金(No.21471011)和北京市高层次人才引进项目资助。

*通信联系人。E-mail:yusy@ruc.edu.cn,jxf19821023@bjut.edu.cn

Pyrazolate-based complexes have caught a plenty of attention not only for their structural diversity, such as clusters[1-2], metallomacrocycles[3-7], metal-oraganic cages[8-9], but also for their physico-chemical properties[10-11] and potential application in the field of organocatalysis, biological mimicry, magnetic coupling, electron transfer, opto-electronicmaterials, *etc*[12]. In our group, we have reported a series of mutifunctional pyrazole-based ligands using as linker and corresponding well-defined metallosupramolecular quantitatively assembled via coordination reaction between pyrazolate linker and dimetal corners $[M_2(bpy)_2(NO_3)_2](NO_3)_2$ or $[M_2(phen)_2(NO_3)_2](NO_3)_2$ (M=Pd)[8-9].

Meanwhile, the transition metal palladium complexes have been a hot topic in the area of Suzuki-coupling reaction. Especially, the mononuclear palladium catalysis had played a crucial role in synthetic organic chemistry for Suzuki-coupling reaction. Although mononuclear palladium catalysis has historically dominated the field, the explorations of Pd … Pd bond-containing complexes′ using as catalysts for Suzuki-coupling reaction, are fleetly in progress and become popular for its unique advantages[13-15].

Based on the numerous advantages of pyrazolate-based complexes and the promising catalyst activity of Pd…Pd bond-containing complexes, it is necessary to study the catalytic activity of pyrazolate-based dipalladium(Ⅱ) complexes with weak intramolecular Pd … Pd bonding interaction, as an important and fascinating subclass of palladium coordination.

Herein, we design the solution synthesis of the pyrazolyl ligand HL[16-17] (Scheme 1) and dipalladium (Ⅱ, Ⅱ) clips to get three new Pd…Pd bond-containing clips (Scheme 2), which have been developed and applied into Suzuki-coupling reactions. Excitedly, we find that the Pd … Pd bond-containing clips whose anion have been changed into PF_6^- show good catalysis properties for Suzuki-coupling reaction although the Pd(Ⅱ) has been coordinated by four inactive N atoms. In addition, all of the complexes have been intensively studied by NMR, ESI-MS, and X-Ray single-crystal diffraction analysis. Interestingly, X-Ray single-crystal diffraction analysis reveals charming structures that the clips not only have weak intramolecular Pd … Pd bonding interaction, but also have chiral axis and F… H hydrogen bond.

1 Experimental

1.1 Materials and instruments

All reagents for synthesis and analysis were obtained commercially with analytical grade and used without further purification and was carried out in the laboratory atmosphere unless reported otherwise. $[Pd_2(bpy)_2L_2](PF_6)_2$ (**1**·$2PF_6^-$), $[Pd_2(dmbpy)_2L_2](PF_6)_2$ (**2**·$2PF_6^-$), $[Pd_2(phen)_2L_2](PF_6)_2$ (**3**·$2PF_6^-$) were prepared according to the literature procedures[18].

^1H and ^{13}C NMR spectra were recorded on

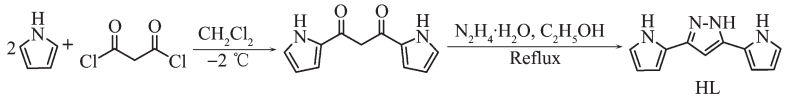

Scheme 1 Synthesis route of ligand HL

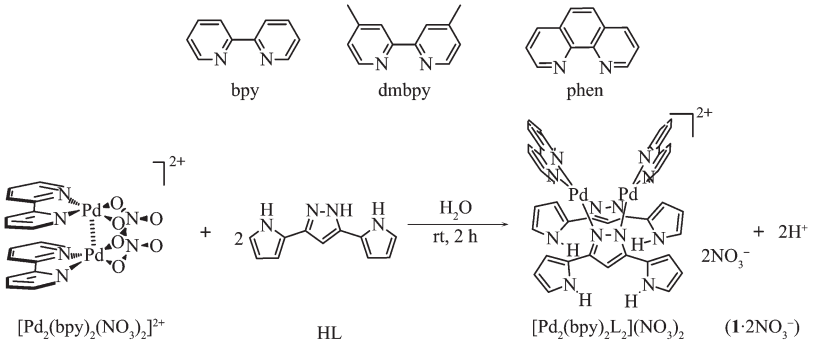

Scheme 2 Synthesis of organometallic “molecular clip”

Bruker AV 400 MHz spectrometers. ESI-MS spectra were recorded on Octant TOF LC-plus 4G mass spectrometer.

1.2 Synthesis and characterization of $1\cdot 2PF_6^-$, $2\cdot 2PF_6^-$ and $3\cdot 2PF_6^-$

1.2.1 General pyrazole ligand preparation

The pyrazole ligand, 3,5-di (2-pyrrolyl)-pyrazole (HL), was synthesized according to a reported procedure (referring to supporting information for the synthesis). ^{1}H NMR (400 MHz, DMSO-d_6, 298 K, TMS): δ 12.65 (s, 1H), 11.23 (s, 1H), 11.12 (s, 1H), 6.85 (s, 1H), 6.71 (s, 1H), 6.55 (s, 1H), 6.48 (s, 1H), 6.28 (s, 1H), 6.11 (s, 1H), 6.05 (d, J=3.0 Hz, 1H) (Fig.S1).

1.2.2 Synthesis and characterization of $[Pd_2(N\hat{}N)_2L_2]^{2+}$-type dimetallo-clips

The self-assembly of bipyrazolate-bridged metallo-clip complex $\mathbf{1}\cdot 2NO_3^-$ was shown in Scheme 2. A mixture of $[Pd_2(bpy)_2(NO_3)_2](NO_3)_2$ (19.3 mg, 0.025 mmol) with HL (9.9 mg, 0.05 mmol) in water resulted in the formation of $\mathbf{1}\cdot 2NO_3^-$ in quantitative yield. A ten-fold excess of KPF_6 was added to the solution to give $\mathbf{1}\cdot 2PF_6^-$ as yellow solid (28.7 mg, Yield 95%). ^{1}H NMR (400 MHz, DMSO-d_6, 298 K, TMS): δ 11.36 (s, 4H), 8.64 (s, 4H), 8.32 (s, 4H), 7.98 (s, 4H), 7.55 (s, 4H), 7.20 (s, 4H), 6.88 (d, J=16.8 Hz, 6H), 5.99 (s, 4H). ^{13}C NMR (400 MHz, DMSO-d_6, 298K, TMS): δ 156.99, 150.88, 147.14, 142.71, 128.22, 124.89, 122.49, 120.56, 109.31, 108.04. Elemental analysis calculated for $C_{42}H_{34}F_{12}N_{12}P_2Pd_2$(%): C: 41.71; H: 2.83; N: 13.90. Found(%): C: 41.65; H: 2.87; N: 13.84. ESI-MS (CH_3CN, m/z): Calcd. for $[\mathbf{1}\cdot PF_6^-]^+$ 1 064.86, Found 1 064.86; $[\mathbf{1}]^{2+}$ 459.95, Found 459.95 (Fig.S2~S4).

The same procedure as employed for $\mathbf{2}\cdot 2PF_6^-$ was followed except that $[Pd_2(dmbpy)_2(NO_3)_2](NO_3)_2$ (20.7 mg, 0.025 mmol) was used as the starting material to give $\mathbf{2}\cdot 2PF_6^-$ as yellow solid (30.3 mg, Yield 96%). ^{1}H NMR (400 MHz, DMSO-d_6, 298 K, TMS): δ 11.34 (s, 4H), 8.52 (s, 4H), 7.82 (d, J=6.0 Hz, 4H), 7.39 (d, J=6.0 Hz, 4H), 7.17 (s, 4H), 6.88 (s, 2H), 6.86 (s, 4H), 6.00 (q, J=2.7 Hz, 4H), 1.06 (s, 12H). ^{13}C NMR (400 MHz, DMSO-d_6, 298K, TMS): δ 156.27, 155.16, 150.11, 147.09, 128.62, 125.47, 122.59, 120.52, 109.30, 107.92, 21.45. Elemental analysis calculated for $C_{46}H_{42}F_{12}N_{12}P_2Pd_2$(%): C: 43.65; H: 3.34; N: 13.28. Found(%): C: 43.58; H: 3.42; N: 13.11. ESI-MS (CH_3CN, m/z): Calcd. for $[\mathbf{2}\cdot PF_6^-]^+$ 1 121.14; Found 1 120.96; $[\mathbf{2}]^{2+}$ 488.07, Found 488.00 (Fig.S5~S7).

The same procedure as employed for $\mathbf{3}\cdot 2PF_6^-$ was followed except that $[Pd_2(phen)_2(NO_3)_2](NO_3)_2$ (20.5 mg, 0.025 mmol) was used as the starting material to give $\mathbf{3}\cdot 2PF_6^-$ as yellow solid (28.9 mg, Yield 92%). ^{1}H NMR (400 MHz, DMSO-d_6, 298 K, TMS): δ 11.43 (d, J=2.9 Hz, 4H), 8.92 (dd, J=8.3, 1.3 Hz, 4H), 8.36 (dd, J=5.4, 1.3 Hz, 4H), 8.25 (s, 4H), 7.88 (dd, J=8.3, 5.4 Hz, 4H), 7.28 (ddd, J=3.9, 2.6, 1.5 Hz, 4H), 7.03 (s, 2H), 6.88 (td, J=2.7, 1.4 Hz, 4H), 5.94 (dt, J=3.6, 2.4 Hz, 4H). ^{13}C NMR (400 MHz, DMSO-d_6, 298 K, TMS): δ 151.78, 147.48, 141.53, 131.00, 128.18, 126.69, 122.59, 120.61, 109.33, 108.34, 102.33. Elemental analysis calculated for $C_{52}H_{48}F_{12}N_{14}O_2P_2Pd_2$(%): C: 44.49; H: 3.45; N: 13.97. Found(%): C: 44.37; H: 3.52; N: 13.83. ESI-MS (CH_3CN, m/z): Calcd. for $[\mathbf{3}\cdot PF_6^-]^+$ 1 112.08; Found 1 112.87; $[\mathbf{3}]^{2+}$ 483.05, Found 482.96 (Fig.S8~S10).

1.3 X-ray crystallography of complex $1\cdot 2PF_6^-$, $2\cdot 2PF_6^-$ and $3\cdot 2PF_6^-$

The intensity data collections for $\mathbf{1}\cdot 2PF_6^-$~$\mathbf{3}\cdot 2PF_6^-$ (Crystal size / mm: 0.10×0.11×0.15 for complex $\mathbf{1}\cdot 2PF_6^-$; 0.12×0.18×0.23 for complex $\mathbf{2}\cdot 2PF_6^-$; 0.11×0.15×0.23 for complex $\mathbf{3}\cdot 2PF_6^-$) were performed on the Bruker Smart APEX Ⅱ CCD diffractometer equipped with graphite monochromated Mo $K\alpha$ radiation (λ= 0.071 073 nm) at (150±2) K. The empirical absorption corrections were applied by using the SADABS program[19]. The structures were solved by direct methods and refined by full matrix least-squares fitting on F^2 by SHELXTL-2014[20]. All non-hydrogen atoms were refined anisotropically. The hydrogen atoms of organic ligands were located geometrically and fixed isotropic thermal parameters. Hydrogen atoms were included in idealized positions with isotropic displacement parameters constrained to 1.5 times the U_{eq} of their attached carbon atoms for methyl hydrogens, and 1.2 times the U_{eq} of their attached carbon atoms for all others. SQUEEZE option was used for the final refinement in order to treat the disordered counter anions and solvent molecules.

The details of data with unit cell, space group, data collection, and refinement parameters are presented in Table 1 and Table S1~S3.

CCDC: 1519041, **1**·2PF_6^-; 1536149, **2**·2PF_6^-; 1536150, **3**·2PF_6^-.

1.4 Catalytic activity test

To explore the catalyst activity of pyrazolate-based dipalladium(Ⅱ) complexes with weak intramolecular Pd⋯Pd bonding interaction, different reaction conditions have been tried to obtain the feasible solution.

In a typical experiment, the iodobenzene (204 mg, 1 mmol), benzeneboronic acid (136 mg, 1 mmol) and K_3PO_4 (636 mg, 3 mmol), **1**·2PF_6^- (12 mg, 10 μmol) or **2**·2PF_6^- (12 mg, 10 μmol) or 3·2PF_6^- (12 mg, 10 μmol)) was added into a 250 mL two-necked flask. Under argon atmosphere, 1,4-dioxane (100 mL) was added, and the suspension was stirred at 100 ℃. After the reactant disappeared (2 days, monitored the consumption of the starting iodobenzene by TLC), the mixture was cooled to room temperature. The reaction mixture was directly filtered and dried to get crude product (90% purity), than through column chromatograph eluting with hexane to give the expected compound (141 mg, Yield 88%) as a white solid. ^{1}H NMR (400 MHz, chloroform-d , 298 K, TMS): δ 7.57 (d, J= 7.3 Hz, 2H), 7.49 (d, J=8.0 Hz, 2H), 7.42 (t, J=7.6 Hz, 2H), 7.32 (t, J=7.3 Hz, 1H), 7.27~7.23 (m, 2H), 2.39 (s, 3H).

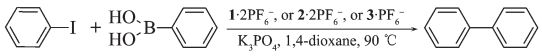

Scheme 3 Catalytic activity of Suzuki cross-coupling reactions

Table 1 Crystal structure determination data for complexes 1·2PF_6^-, 2·2PF_6^- and 3·2PF_6^-

Complex	**1**·2PF_6^-	**2**·2PF_6^-	**3**·2PF_6^-
Formula	$C_{42}H_{34}F_{12}N_{12}P_2Pd_2$	$C_{46}H_{42}F_{12}N_{12}P_2Pd_2$	$C_{52}H_{48}F_{12}N_{14}O_2P_2Pd_2$
Formula weight	1 209.55	1 265.66	1 403.78
Crystal system	Monoclinic	Monoclinic	Monoclinic
Space group	$P2_1/c$	$P2_1/c$	$C2/c$
a / nm	1.800 80(10)	2.539 39(17)	2.908 4(2)
b / nm	1.832 34(11)	1.889 80(13)	1.049 38(7)
c / nm	1.786 63(10)	2.831 36(17)	2.126 16(18)
β / (°)	100.802(2)	105.883(2)	115.122(5)
Volume / nm^3	5.790 8(6)	13.06 88(15)	5.875 3(8)
Z	4	8	4
D_c / (g·cm^{-3})	1.387	1.286	1.587
μ / mm^{-1}	0.753	0.670	0.757
F(000)	2 400	5 056	2 816
Index ranges	$-26 \leqslant h \leqslant 26$, $-25 \leqslant k \leqslant 27$, $-22 \leqslant l \leqslant 26$	$-31 \leqslant h \leqslant 31$, $-23 \leqslant k \leqslant 22$, $-35 \leqslant l \leqslant 35$	$-36 \leqslant h \leqslant 36$, $-13 \leqslant k \leqslant 13$, $-26 \leqslant l \leqslant 26$
2θ range / (°)	4.6~65.0	4.4~52.8	5.0~53.0
Reflections collected	136 602	238 460	42 160
Observed reflections with ($I>2\sigma(I)$)	14 672	20 057	5 574
Number of parameters	631	1 341	381
Independent reflections	20 911 (R_{int}=0.197 1)	26 924 (R_{int}=0.262 4)	6 076 (R_{int}=0.145 6)
Goodness-of-fit on F^2	1.04	1.04	1.08
Final R indices ($I>2\sigma(I)$)	R_1=0.055 8, wR_2=0.146 9	R_1=0.099, wR_2=0.242	R_1=0.056, wR_2=0.154
R indices (all data)	R_1=0.075 0, wR_2=0.154 9	R_1=0.123 0, wR_2=0.260 5	R_1=0.058 1, wR_2=0.157 3
Largest diff. peak and hole / (e·nm^{-3})	2 245 and −2 006	2 370 and −2 962	1 863 and −2 170

2 Results and discussion

2.1 Characterization of $[Pd_2(N\hat{}N)_2L_2]^{2+}$-type dimetallo-clips

Complexes $\mathbf{1}\cdot 2PF_6^-$, $\mathbf{2}\cdot 2PF_6^-$ and $\mathbf{3}\cdot 2PF_6^-$ were fully characterized by NMR and ESI-MS. The NMR spectrum of $\mathbf{1}\cdot 2PF_6^-$ clearly shows that a 1:1 Pd(bpy) to L^- complex was formed (Fig.S2). As shown in ^1H NMR of $\mathbf{1}\cdot 2PF_6^-$ (Fig.S2), two N-protons of the ligand in the product turned out to be only one singlet at δ 11.36, which presents two singlets at 11.24 and 11.12 for H6 and H6′, respectively, before self-assembly (see synthesis part). This can only be explained by that the N-protons of the ligand in the complex HL were equivalent. In addition, the resonance signals of the CH of two pyrrole rings changed from a pair single peak into a multiple peak. Moreover, the assignment of product $\mathbf{1}\cdot 2PF_6^-$ as dimetallo-clip $[Pd_2(N\hat{}N)_2L_2]^{2+}$-type dimetallo-clip is further proved by ESI-MS studies, where multiply charged molecular ions corresponding to intact dimetallo-clip were observed. The ESI-MS experiment was performed in acetonitrile solution. As shown in Fig.S4, the multiply charged molecular ions of $\mathbf{1}\cdot 2PF_6^-$ at *m/z* 1 064.86 and 459.95 are ascribed to the cations of $[\mathbf{1}\cdot PF_6^-]^+$, $[\mathbf{1}]^{2+}$, respectively. The other two similar complexes $\mathbf{2}\cdot 2PF_6^-$ and $\mathbf{3}\cdot 2PF_6^-$ are also obtained and characterized by the same method (Fig. S5~S10). All the characterizitions have demonstrated that the preparaton of these organometallic clips as mentioned is successful. The solid state structures of these "molecular clips" have been further confirmed by single-crystal X-ray diffraction analysis.

2.2 Crystal structures of the dimetallo-clips

Single crystals of $\mathbf{1}\cdot 2PF_6^-$, $\mathbf{2}\cdot 2PF_6^-$ and $\mathbf{3}\cdot 2PF_6^-$ were obtained by vapor diffusion of diethyl ether into their acetonitrile solutions. Their corner-like structure are strongly supported by single-crystal structure analysis.

An ORTEP representation of $\mathbf{1}\cdot 2PF_6^-$ is shown in Fig.1 and selected bond lengths and bond angles are listed in Table S1. The complex $\mathbf{1}\cdot 2PF_6^-$ crystallizes in the monoclinic space group $P2_1/c$. The crystal structure analysis for $\mathbf{1}\cdot 2PF_6^-$ reveals a Pd_2 dimetallic corner-shaped structure with one (μ-pyrazolato-N,N')$_2$ doubly bridged [Pd(bpy)]$_2$ dimetal corner. The $[Pd_2L_2]$-tpye corner is constituted by two monopyrazole ligands L and two Pd(bpy) motifs. The central six membered ring consisting of the two Pd atoms and the four pyrazolyl N atoms has a boat-shaped conformation with Pd-N_{pz} distances between 0.200 41(18) and 0.202 82(19) nm. The two pyrazole rings form a dihedral angle of 92.14° and form dihedral angles of about 5.65°, 15.71°, 35.89° and 39.53° with pyrrole planes in the pyrazole bridged ligand. The dihedral angle between the two bpy ligands in the corner is 65.53°, which is smaller than the dihedral angle between the pyrazolate ligands. The distance of Pd1-Pd2 is 0.311 79 (3) nm which is in the range of typical Pd⋯Pd interactions (0.26~0.33 nm) [3] and reveals weak Pd⋯Pd interaction. As shown in Fig.2, in the solid crystal structure, a 1D helical chain with the pitch of 0.916 nm along the *b* axis is constructed through multiple intermolecular C–H⋯F, N–H⋯F hydrogen bonds between dimetallo-clip cation and counter anions and intermolecular $\pi\cdots\pi$ packing interaction between bpy ligands. Furthermore, an anionic channel along crystallographic *c* axis exist in crystal structure. A 2D supramolecular network structure is showed in Fig.2b.

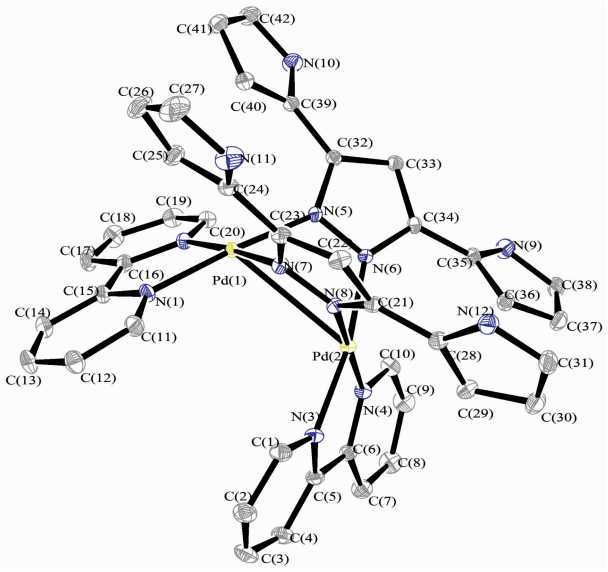

Thermal ellipsoids are shown at the 30% probability level; Counter anions and hydrogen atoms are omitted for clarity

Fig.1 ORTEP diagram of the molecular structure of $\mathbf{1}\cdot 2PF_6^-$

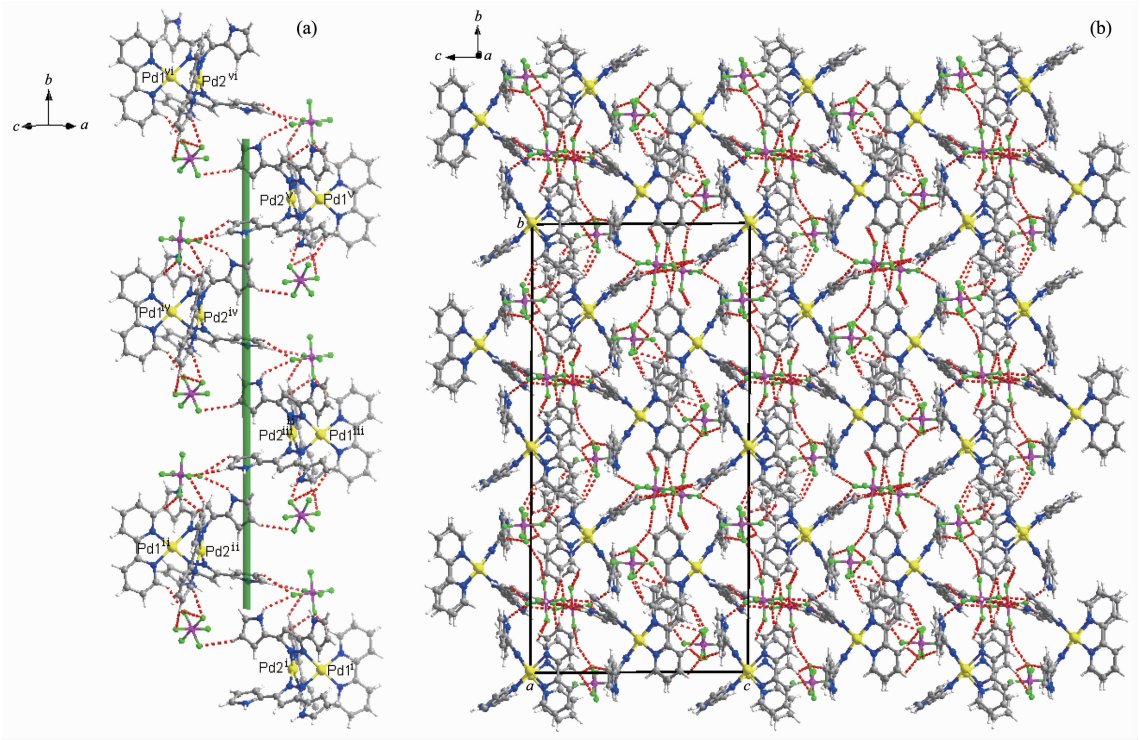

Hydrogen bonds are shown as dashed lines; Symmetric code: [i] 1+*x*, −0.5−*y*, −0.5+*z*; [ii] 1−*x*, −*y*, −*z*; [iii] 1+*x*, −0.5−*y*, −0.5+*z*; [iv] 1−*x*, 1−*y*, −*z*; [v] 1+*x*, 1.5−*y*, 0.5+*z*; [vi] 1−*x*, 2−*y*, −*z*

Fig.2 (a) 1D helix chain along *b* axis; (b) Crystal packing as seen along *c* axis

An ORTEP representation of **2**·2PF_6^- is shown in Fig.S14 and selected bond lengths and bond angles are listed in Table S2. The complex **2**·2PF_6^- crystallizes in the monoclinic space group $P2_1/c$. The crystal structure analysis for **2**·2PF_6^- also display a Pd_2 dimetallic corner-shaped structure with one (μ-pyrazolato-*N*,*N*′)$_2$ doubly bridged [Pd(dmbpy)]$_2$ dimetal corner similar to that of **1**·2PF_6^-. The dihedral angle between the dmbpy ligands in the corner is 67.3°, which are significantly larger than those of **1**·2PF_6^-. The separations of Pd⋯Pd (0.308 28(8) nm) is comparable to those of **1**·2PF_6^- and also indicate weak Pd⋯Pd interactions. The two pyrazole rings form a dihedral angle of 67.32° and form dihedral angles of about 3.89°, 6.25°, 10.85° and 37.19° with pyrrole planes in the pyrazole bridged ligand, which are significantly smaller than those of **1**·2PF_6^-. In the crystal, molecules of complex **2**·2PF_6^- pack by multiple intermolecular C–H⋯F, N–H⋯F hydrogen bonds between dimetal corner cations and counter anions, intermolecular $\pi\cdots\pi$ packing interaction and intermolecular C–H⋯π bonds between neighboring molecules, which built a 1D helical chain with the pitch of 0.946 nm along the *b* axis and a 2D supramolecular network structure shown in Fig.S15.

An ORTEP representation of **3**·2PF_6^- is shown in Fig.S16 and selected bond lengths and bond angles are listed in Table S3. The complex **3**·2PF_6^- crystallizes in the monoclinic space group *C*2/*c*. As shown in Fig.S16, the crystal structure analysis for **3**·2PF_6^- reveals a Pd_2 dimetallic corner-shaped structure with one (μ-pyrazolato-*N*,*N*′)$_2$ doubly bridged [Pd(phen)]$_2$ dimetal corner. In the dipalladium corner, the dihedral angles between the two pyrazolate planes is 98.18°, and the two pyrazole rings form dihedral angles of about 2.49°, 2.49 °, 21.05° and 21.05° with pyrrole planes in the pyrazole bridged ligand. The dihedral angle between the phen ligands within the dimetal corners is 51.9°, which is obviously smaller than those of **1**·2PF_6^- and **2**·2PF_6^-. The separation of Pd1⋯Pd#1 (0.303 00(5) nm) is slightly shorter than the sum of the van der Waals radii of palladium, indicating the presence of weak Pd⋯Pd interactions. Multiple

intermolecular C–H⋯F, N–H⋯F hydrogen bonds between dimetal corner cations and counter anions and intermolecular C–H⋯π bonds between neighboring molecules construct a 1D helical chain with the pitch of 0.525 nm along the *b* axis and a 2D supramolecular network structure is shown in Fig.S17.

2.3 Catalytic activity

We were pleased to find that the reaction proceeded smoothly in refluxing 1,4-dioxane for 48 h to provide product biphenyl in good yields (Table 2). But it could not be further improved as increasing the ratio of **1**·2PF_6^- (**2**·2PF_6^-, or **3**·2PF_6^-).

With the optimal reaction conditions (1∶1 of n_A∶n_B, K_3PO_4, 1%(*n*/*n*) catalyst, 1,4-dioxane, at 90 ℃) in hand, the reactions of A with various boric acid derivatives were explored to gauge the generality of this process (Table 3). For the substrates bearing electron-donating (-OMe, -CH_3) and electron-withdrawing groups (-CHO) on the phenyl ring (R_1, R_2), the reactions proceeded smoothly to give the corresponding biphenyl compounds $\mathbf{C}_1$ in 78%~88% yields, $\mathbf{C}_2$ in 60%~78% yields, $\mathbf{C}_3$ in 56%~76% yields. In addition, electron-donating (-OMe, -CH_3) boric acids tend to have higher yields than electron-withdrawing groups (-CHO) boric acids during the reactions. The reasons of the difference yields of $\mathbf{C}_1$ ($\mathbf{C}_2$, or $\mathbf{C}_3$) may be the different steric effect of **1**·2PF_6^- (**2**·2PF_6^- or **3**·2PF_6^-) during the reactions.

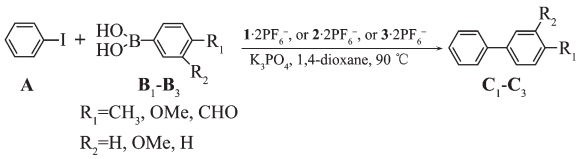

Scheme 4

Table 2　Catalytic activity of complexes 1·2PF_6^-, 2·2PF_6^- and 3·2PF_6^-

Entry	Catalyst	Co-catalyst	Solvent	*T* / ℃	Time / h	Yield /%
1	**1**·2PF_6^-	K_3PO_4	1,4-dioxane	90	48	95
2	**2**·2PF_6^-	K_3PO_4	1,4-dioxane	90	48	93
3	**3**·2PF_6^-	K_3PO_4	1,4-dioxane	90	48	88

Table 3　Catalytic activity of complexes 1·2PF_6^-, 2·2PF_6^- and 3·2PF_6^-

Entry	Catalyst	R_1	R_2	Product	Yield / %
1	**1**·2PF_6^-	CH_3	H	$\mathbf{C}_1$	88
2		OMe	OMe	$\mathbf{C}_2$	78
3		CHO	H	$\mathbf{C}_3$	76
4	**2**·2PF_6^-	CH_3	H	$\mathbf{C}_1$	85
5		OMe	OMe	$\mathbf{C}_2$	74
6		CHO	H	$\mathbf{C}_3$	70
7	**3**·2PF_6^-	CH_3	H	$\mathbf{C}_1$	78
8		OMe	OMe	$\mathbf{C}_2$	60
9		CHO	H	$\mathbf{C}_3$	56

3 Conclusions

In summary, of three Pd⋯Pd bond-containing complexes are synthesized via a directed coordination driving approach that occurs along with spontaneous deprotonation of the ligand and three organometallic "molecular clips" (M_2L_2) are generated in nearly quantitative yield. All of the structures are characterized by ^{1}H NMR, ^{13}C NMR, ESI-MS, and single-crystal X-ray diffraction analysis. More interestingly, pyrazolate-based dipalladium (Ⅱ) clips with weak intra-molecular Pd⋯Pd bonding interaction which are coordinated by four inactive N atoms exhibit good catalytic activity for Suzuki-coupling reaction.

Acknowledgments: This project was supported by the National Natural Science Foundation of China (No.91127039, 21471011) and the Importation and Development of High-Caliber Talents Project of Beijing Municipal Institution.

Supporting information is available at http://www.wjhxxb.cn

References:

[1] Ahmed B M, Gellert M. *Inorg. Chem.*, **2016**,**55**:7717-7728

[2] Nicola C D, Garau F, Gazzano M, et al. *Cryst. Growth Des.*, **2015**,**15**:1259-1272

[3] Yu S Y, Huang H P, Li S H, et al. *Inorg. Chem.*, **2005**,**44**: 9471-9488

[4] Ning G H, Yao L Y, Liu L X, et al. *Inorg. Chem.*, **2010**,**49**: 7783-7792

[5] Ning G H, Xie T Z, Pan Y J, et al. *Dalton Trans.*, **2010**,**39**: 3203-3211

[6] Xie T Z, Guo C, Yu S Y, et al. *Angew. Chem. Int. Ed.*, **2012**, **51**:1177-1181

[7] Tong J, Yu S Y, Li H. *Chem. Commun.*, **2012**,**48**:5343-5345

[8] Yu S Y, Jiao Q, Li S H, et al. *Org. Lett.*, **2007**,**9**:1379-1382

[9] Jiang X F, Deng W, Jin R, et al. *Dalton Trans.*, **2014**,**43**: 16015-16024

[10]Fujisawa K, Ishikawa Y, Miyashita Y, et al. *Inorg. Chim. Acta*, **2010**,**363**:2977-2989

[11]Sun Q F, Liu L X, Huang H P, et al. *Inorg. Chem.*, **2008**, **47**:2142-2154

[12]La Monica G, Ardizzoia G A. *Progress in Inorganic Chemistry*: *Vol.*46. Karlin K D. Ed. New York: Wiley, **1997**:151-238

[13]Ogura T, Yoshida K, Yanagisawa A, et al. *Org. Lett.*, **2009**, **11**:2245-2248

[14]Baya M, Houghton J, Konya D, et al. *J. Am. Chem. Soc.*, **2008**,**130**:10612-10624

[15]Oldenhof S, Lutz M, Bruin B, et al. *Organometallics*, **2014**, **33**:7293-7298

[16]Hassner A, Fogler E. *Heterocycles*, **2009**,**77**:301-309

[17]Huang H P, Li S H, Yu S Y, et al. *Inorg. Chem. Commun.*, **2005**,8:656-660

[18]HU Jia-Hua(胡佳华), DENG Wei(邓威), JIANG Xuan-Feng (蒋选丰), et al. *Chinese J. Inorg. Chem.*(无机化学学报), **2015**,**31**:1278-1286

[19]Sheldrick G M. *SADABS*, University of Göttingen, Germany, **1996**.

[20]Sheldrick G M. *SHELXTL*-2014, Madison, Wisconsin, USA: Siemens Analytical X-ray Division, **2014**.